# Diagnostics for mechanical heating in star-forming galaxies

Kazandjian, M.V

**Author**: Kazandjian, Mher V.
**Title**: Diagnostics for mechanical heating in star-forming galaxies
**Issue Date**: 2015-06-03

# I

# Introduction

Matter between the stars occupies most of the volume of galaxies and it is referred to as the interstellar medium (ISM). The ISM comprises mainly of gas and dust. Part of the remaining volume is occupied by stars. In addition to these, it is believed that dark matter is a major component of a galaxy, but we will not refer to it in this thesis. Interstellar gas densities range from $10^{-3}$ cm$^{-3}$ at the outer edge of a galaxy near the intergalactic medium (Bregman 2007), up to $10^{10}$ cm$^{-3}$ in proto-planetary disks (Mac Low & Klessen 2004). However, most of this gas is in the 0.3 to 30 cm$^{-3}$ range (Draine 2010).

The ISM represents about 10% of the total mass of a spiral galaxy. On average 1% of the mass of the ISM is in the form of dust. Different densities and thermal conditions are found in the ISM. Various phases have been recognized in the ISM (Wolfire et al. 1995, Tielens 2005, Snow & McCall 2006). The properties of these phases are summarized in Table-1.1. The subject of study in this thesis will be the molecular ISM.

Stars are easy to observe since they emit brightly in the visible range of the electromagnetic spectrum, but detection of the gas is not as easy. The various species can be detected and distinguished by analyzing the emission or absorption spectra of the various transitions among their discrete quantum states. In order for the emission of the gas to be observed, the species in the gas should be excited, so that the various transitions among these internal states can occur; eventually the photons emitted from these transitions are detected by our telescopes. To give a general idea of the sizes of the objects involved: the typical length scale of a galaxy is on the order of 10 to 100 kpc whereas the sizes of molecular clouds, where star formation occurs, range between 0.1 and 100 pc.

| phase | density ($cm^{-3}$) | temperature (K) | volume filling factor |
|---|---|---|---|
| Hot ionized medium | $\sim 3 \times 10^{-3}$ | $\sim 5 \times 10^5$ | $0.5^{\dagger}$ |
| Warm ionized medium | $\sim 0.3$ | $\sim 10000 - 8000$ | 0.1 |
| Warm neutral medium | $\sim 0.3$ | $\sim 8000$ | 0.4 |
| Cold neutral medium | $\sim 30$ | $\sim 50$ | 0.01 |
| Diffuse molecular clouds | $> 100 - 500$ | $\gtrsim 25 - 100$ | $\sim 10^{-3}$ |
| Dense molecular clouds | $> 10^4$ | $\gtrsim 10 - 50$ | $< 10^{-4}$ |

Table 1.1 – Typical gas densities and kinetic temperatures of the phases of the ISM (Tielens 2005, Draine 2010).
$^{\dagger}$ The volume filling factor for this phase of the ISM is uncertain (Draine 2010).

## 1.1 Chemistry and radiation

Most of the gas of the ISM is in the form of ionized hydrogen, HII, in the hot and warm ionized media. Neutral hydrogen, HI, is found in the warm neutral and the cold neutral media (labeled with the acronyms CNM and WNM, respectively, see Table-1.1). H is the simplest species in the ISM and it is the essential ingredient to form molecular hydrogen $H_2$. The formation of $H_2$ takes place mostly on the surface of dust grains (Gould & Salpeter 1963). Regions of the interstellar medium where the bulk of hydrogen is in the form of $H_2$ are known as molecular clouds. $H_2$ does not have a permanent electric dipole moment, since it is formed of two identical H atoms. Thus, it can not emit due to $\Delta J = \pm 1$ transitions, which are strictly forbidden. On the other hand $H_2$ does have a quadrupole moment which allows for $\Delta J = \pm 2$ transitions. The energy of these transitions is quite high, the least energetic of which is the $J = 2 - 0$ with $E/k_b = 512$ K, which renders its emission too weak in environments such as molecular clouds where the temperatures are too low (Shull & Beckwith 1982, Stahler & Palla 2005). The molecular ISM is mostly cold ($\sim$ 10 K ) and dense (see Table-1.1), hence the gas is prone to gravitational instabilities which induce the clumpy and filamentary structure in the molecular ISM (Larson 1981, Falgarone & Phillips 1990, de Vega et al. 1996); it is believed that stars are born in these unstable regions. To have a good understanding of the overall mechanisms regulating galaxy formation and evolution it is essential to have a deep knowledge of the underlying physics and chemistry of star-forming regions.

Visible light in molecular clouds is highly obscured by dust. Infrared radiation emitted by the dust in these clouds can penetrate large column densities of $H_2$ ( $N(\mathrm{H}) \gtrsim 10^{24}$ cm$^{-3}$) and is used instead of visible light to study star forming regions.

The far-ultraviolet (FUV) radiation (6 < E < 13.6 eV) of stars heats the gas surrounding them and excites the internal energy levels of H gas. Regions of the ISM which are dominated by such radiation and where the gas changes from ionized to neutral to molecular are called "photon-dominated regions" (Tielens & Hollenbach 1985). A schematic diagram of a typical PDR showing the important chemical transitions, is shown in Figure-1.1

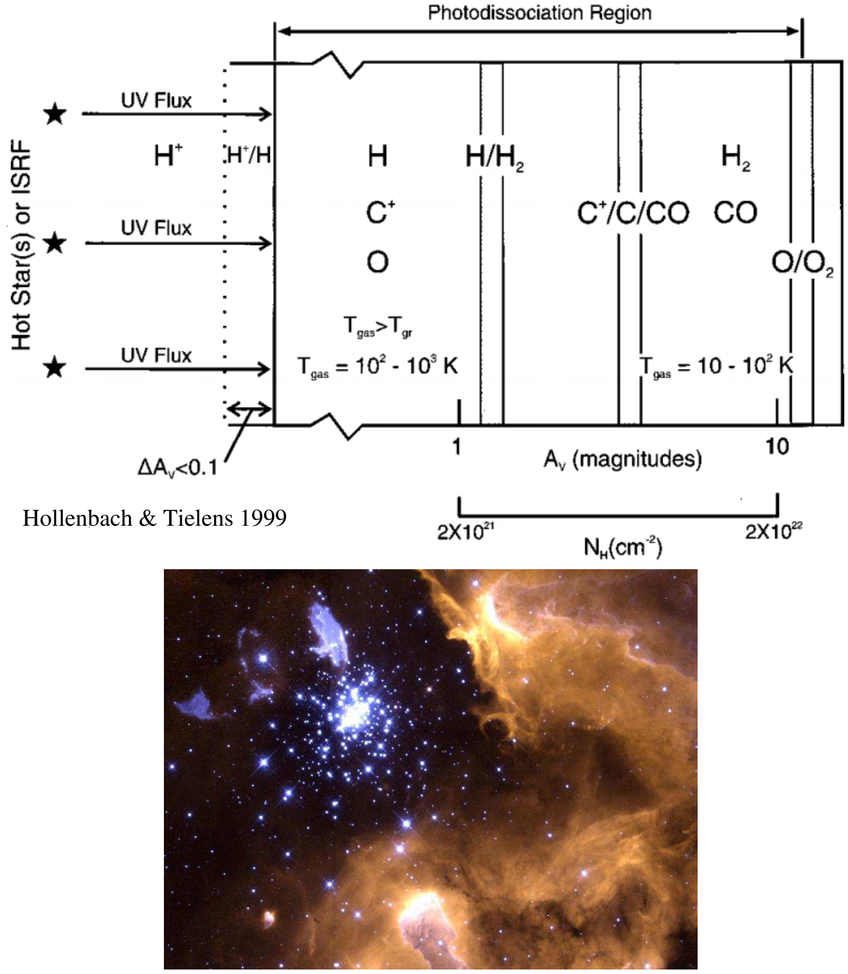


Figure 1.1 – *Top*: schematic diagram of a PDR; *bottom*: HST image of the nebula NGC 3603. NASA, Wolfgang Brandner (JPL/IPAC), Eva K. Grebel (Univ. Washington), You-Hua Chu (Univ. Illinois Urbana-Champaign)

In PDRs the surface layer of the clouds is heated by FUV and ionized by extreme ultraviolet (EUV, 13.6 eV < E < 0.1 keV) photons. The flux of these photons is rapidly attenuated at greater columns of hydrogen ($N$(H)), where the temperatures decrease. As the kinetic temperature decreases, ionized hydrogen, $H^+$, recombines with free electrons to form neutral hydrogen, HI. At higher column densities HI is transformed into $H_2$ via gas-grain processes. The dust catalyzes the formation of $H_2$ via a three-body process, two HI atoms and the dust grain. An HI atom has a certain probability of sticking on the surface of a dust grain. Once on the surface, it can recombine with another HI atom which is also wandering on the surface to form $H_2$, which then leaves the surface of the grain (Gould & Salpeter 1963). In fact, the direct recombination of two hydrogen atoms in the gas phase is a very slow process compared to the three-body processes[1]. In the shielded region of the cloud, where the flux of FUV photons is progressively more diluted relative to the surface, molecular species other than $H_2$ form. Many species have been detected: see for instance the review by Tielens (2013). Most commonly observed in the sub-millimeter and the infrared wavelengths are species such as CO, $^{13}$CO, HCN, HNC, $HCO^+$, CS, CN, SiO, $H_2O$, where CO is the most abundant species. The energy levels of these species are excited by collisions with $H_2$ (para- and ortho-) in addition to H, He, $H^+$, $e^-$. It should be noted that excitation due to the collisions with the last two partners is less significant in the shielded region of the PDR because of the low ionization fraction in these environments (Tielens & Hollenbach 1985), and is relevant in environments with enhanced ionization due to for example X-rays (Maloney et al. 1996b) or cosmic rays (Papadopoulos 2010). The excited population levels eventually tend to decay to lower energy states by spontaneous radiative emission. The densities of the colliding species necessary to excite the higher transitions and consequently to enable emission to be observed depend on their radiative properties. At local thermal equilibrium (LTE) the population densities of the levels between which the transition occurs are determined by the partition function. Usually LTE population densities are achieved whenever the density of the colliding species >> $n_{\rm crit}$, where $n_{\rm crit}$ is the critical density defined as $n_{\rm crit} \equiv A_{ij}/K_{ij}$ (cf. Tielens 2005); $K_{ij}$ is the collisional rate coefficient of the transition from the $i^{th}$ to the $j^{th}$ level and $A_{ij}$ is the spontaneous de-excitation rate, the Einstein A coefficient[2]. Generally, the ISM is not in LTE because $n < n_{\rm crit}$. Thus, a good knowledge of the intensities of the emission provides insight on the underlying physical excitation mechanisms of the species (van der Tak 2011).

The main heating mechanism in PDRs is photo-electric heating, which is the heating of the gas due to the photo-electric effect on dust grains. Electrons ejected due to absorption by FUV photons in these grains collide elastically with the gas and heat it up (Bakes & Tielens 1994). This is the mechanism through which the gas, the FUV radiation and the dust are coupled to each other. In this thesis we do not focus on modeling HII regions since the medium is fully ionized and no molecules are present; this renders HII regions irrelevant for the molecular emission we are interested in. Cosmic rays can also play an important role in the heating of the gas in the UV-shielded region of the cloud. It has been proposed that the cosmic ray ionization rate in extreme star-burst regions could be as high as $10^4$ times the ionization rate of the solar neighborhood (Papadopoulos 2010, Meijerink et al. 2011, Ao et al. 2013). These regions are referred to as cosmic-ray dominated regions (CRDRs). Moreover, in active galactic nuclei, X-ray heating is also potentially important. Similar to cosmic rays, energetic X-rays can penetrate through large columns of HI and $H_2$ ($N$(H) $\gtrsim 10^{24}$ cm$^{-3}$) and heat up the gas in the regions where FUV photons

[1] In the chemistry of the early Universe, the only channel for the formation of $H_2$ are gas phase reactions, in particular the so-called $H_2^+$ and $H^-$ channels (Abel et al. 1997, Galli & Palla 1998, Lepp et al. 2002, Coppola et al. 2011). The former consists on the charge transfer between $H_2^+$ and H and the latter is represented by the associative detachment of H and $H^-$

[2] See Krumholz 2007 for the modified definition of the critical density which takes self-shielding into account

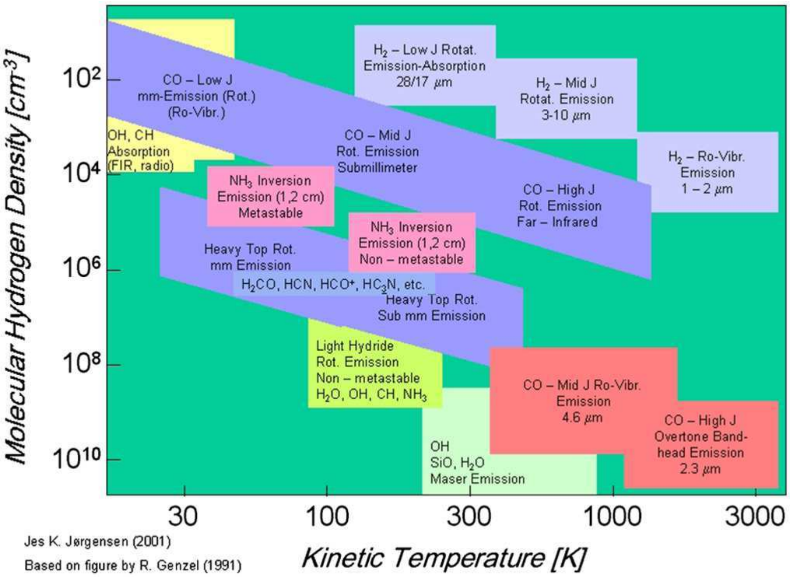


Figure 1.2 – Temperatures and density ranges in the ISM probed by some molecular lines. This diagram is taken from Tielens (2013) which in turn is a modified version from Genzel (1991) and is provided by Jes Jørgensen.

are shielded. These regions are referred to as X-ray dominated regions (XDRs: Maloney et al. 1996a, Bradford et al. 2003, Meijerink & Spaans 2005, Papadopoulos et al. 2011, Bayet et al. 2011, Meijerink et al. 2011). Unlike a PDR where the thermal and chemical properties vary steeply as a function of the column density of $H_2$ (see left panel of Figure-1.1), in XDRs and CRDRs a decrease in temperature and ionization is realized throughout these regions. In addition to the three excitation mechanisms discussed above, we will demonstrate in this thesis that mechanical feedback plays an important role in the thermal budget of PDRs which are at chemical and thermal equilibrium. So far we have only mentioned the important heating mechanisms in PDRs. Thermal equilibrium is achieved through fine structure line cooling of atomic and ionized species; the most dominant of which are [CII] 158 $\mu$m and [OI] 63 $\mu$m line cooling (Kaufman et al. 1999). For example, observations of 29 extreme star-forming environments by Rosenberg et al. (2015) in the HerCULES survey reveal that [CII] 158 $\mu$m and [OI] 63 $\mu$m contribute up to $\sim$ 70% of the far infrared emission of these galaxies, with a significantly lower contribution by CO (see Table-4 by Rosenberg et al. 2015).

The gas in the ISM can emit at different wavelengths depending on the difference in the energies of the levels involved in the transition. The most important transition types are summarized in Table-1.2.

For instance, the ionization of a hydrogen atom requires 13.6 eV ($\sim$ 160,000 K), corresponding to photons in the EUV spectrum. On the other hand, transitions among

| | Process | Energy [eV] | Example |
|---|---|---|---|
| Atoms | | | |
| | Ionization | $3 \rightarrow 25$ (first ionization) | |
| | Excitation | few$\rightarrow 10$ | |
| | Spin-Spin (HI) | $5.9 \times 10^{-6}$ | |
| Molecules | | | |
| | Dissociation | few | 4.5 eV for $H_2$ |
| | | | 11.2 eV for CO |
| | Vibration | $(10^{-3} \rightarrow 1)$ (infra-red ) | 1 eV for $H_2$ |
| | | | 0.27 eV for CO |
| | Rotation | $< 10^{-2}$ (micro-wave) | 0.04 eV for $H_2$ |
| | | | $4.7 \times 10^{-4}$ eV for CO |

Table 1.2 – Energies for some specific chemical processes (Tielens 2005)

the quantum states of molecular species can be rotational, vibrational and electronic, or various combinations of these. These transitions obey selection rules, that allow for some of them to take place and forbid others. The energies of electronic transitions are on the order of a few eV. Thus, they can be used to probe gas with $T > 10,000$ K. In order to probe lower temperature gas, $T < 100$ K typical for molecular clouds, transitions with low energies must be considered, such as the CO(1-0) rotational transition which has an energy $E_{\rm upper}/k_b = 5.5$ K and a rest frame wavelength of 2.6 $\mu$m, placing it in the sub-mm regime of the electromagnetic spectrum. In Figure-1.2, the species commonly used to probe different ranges in density and temperature are shown.

## 1.2 Star formation, mechanical feedback and turbulence

The distribution of stellar masses is empirically described by a set of power-law functions, referred to as the initial mass function (IMF), which determines the probability of finding a star within a certain mass range. Stellar masses range from $\sim 0.1$ to $\sim 100$ $M_\odot$, where the IMF is a decreasing function of stellar mass (Salpeter 1955, Kroupa 2001). These very hot and very bright massive stars are (much) less numerous than low-mass stars. Although these form about 0.1% of the total stellar population, stars with $M \sim 100$ $M_\odot$ emit about $3 \times 10^4$ times more ionizing photons than stars of lower mass such as the Sun (Avedisova 1979, Sternberg et al. 2003). The ionizing photons from massive stars, particularly in star-forming and star-bursting regions[3], play a very important role in regulating the star formation rate. The pressure feedback from the photo-ionized gas around such stars may drive a thermal wind that can diminish the accretion due to the self-gravity of molecular gas, thus reducing the star formation efficiency and in some extreme cases halting the process of forming new stars (see review by Krumholz 2015).

[3] Star-bursting regions are regions where the star formation rate is very high $> 1$ $M_\odot$ yr$^{-1}$(e.g. Gao & Solomon 2004), compared to the mean estimate of 0.3 $M_\odot$ yr$^{-1}$ in our galaxy (Robitaille & Whitney 2010).

Massive stars are also important because they are very short lived. They detonate as supernovae liberating typically $10^{51}$ ergs per event (Norman & Ferrara 1996). The shock waves of the blast propagate in its surrounding molecular gas, disturbing the ISM and inducing turbulence and providing mechanical feedback (see review by Mac Low & Klessen 2004). A few percent of the energy of a supernova is re-absorbed by the ISM which is heated up. FUV radiation in PDRs, X-rays in XDRs and cosmic rays in CRDRs heat and ionize the ISM locally, where the efficiency of the heating decreases for increasing column densities of H; this attenuation is less efficient for cosmic rays. The main difference between these three types of regions of the ISM, and regions that are mechanically heated by, e.g., supernovae, is that shocks and turbulence in the latter heat the ISM globally on larger scales down to the smallest scales, few pc and up to a kpc. In this thesis, we study the influence of increasing amounts of turbulent heating on the chemical and radiative properties of the ISM in a statistical manner.

## 1.3 Modeling

The modeling of the physical and chemical processes taking place in a galaxy and the comparison of the results to observations represents a major challenge. While the modeling of self-gravitating systems is a relatively well-defined problem, the hydrodynamic modeling with various cooling, heating and chemical processes is not. For instance, uncertainties in the reaction rates of chemical pathways for the formation and destruction of species affect the solution of the ordinary differential equations that describe the time evolution of the fractional abundances. As a consequence, the cooling and heating mechanisms can easily be either under- or over- estimated. Moreover, since about one per cent of the ISM by mass is composed of dust, all the major gas-phase and gas-grain reactions should be taken into account in order to properly describe the chemistry. The fast formation rate of $H_2$ required for its high abundance in the ISM was explained by Gould & Salpeter (1963), who showed that dust catalyzes the reaction of HI on the surface of grains that have a temperature in the range of 5 K – 20 K. The formation efficiency of $H_2$ on grain surfaces is close to unity for $T_{\rm kin} < 20$ K. It decreases to $\sim 0.1 - 0.2$ for $T_{\rm kin} \sim 500$ K which is still efficient for astrophysically relevant conditions in the ISM (Cazaux & Tielens 2002, 2004).

Another more practical challenge in self-consistent realistic modeling of molecular clouds is the computing times (CPU time) presently required. There have been many attempts of understanding the evolution of molecular clouds, but resolved galaxy-scale self-consistent simulations treating the chemical, radiative transfer and thermal processes accurately and simultaneously require prohibitively long CPU time.

## 1.4 The inverse problem and diagnostics

Recovering the physical conditions of the gas of the ISM can be thought of as an inverse problem; where given information on the emission, for example, the observed spectra,

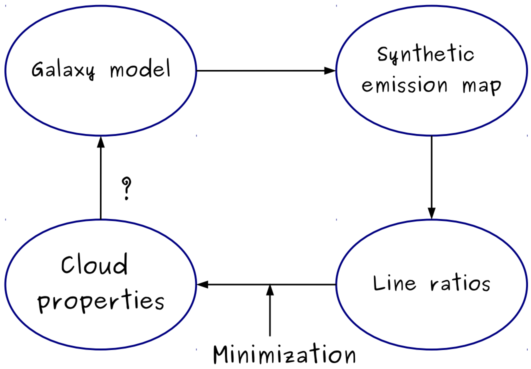


Figure 1.3 – Flow chart diagram of the procedure with which observations are matched to model predictions; The quantity minimized in recovering the “cloud parameters” from the “line ratios” is particular to the approach of this thesis. Any other quantity of interest can be minimized in-order to match the model predictions to the observations.

the challenge is to reconstruct the physical conditions of the gas that have given rise to the observed emission. Unlike the forward modeling process, the inverse problem is not uniquely defined; it tends to suffer from various degeneracies. The general scheme of the modeling procedure is presented in Figure-1.3, where model (or synthetic) emission are computed and compared to observed line ratios for an idealized galaxy; eventually individual cloud properties are recovered.

Computation of the synthetic maps involves the solution of a radiative transfer problem, for an assumed chemistry. The physics and chemistry incorporated in the modeling provide us with different amounts and levels of information, depending on the sophistication of the models and the degree of information and detail with which a galaxy or cloud is studied. For instance, using large-velocity-gradient (LVG) models of the line emission, various authors (e.g. Sobolev 1960, Henkel et al. 1983, Jansen et al. 1994, Hogerheijde & van der Tak 2000, van der Tak et al. 2007, Krumholz 2014) have shown that it is possible to constrain the gas temperature, the density of $H_2$, the velocity gradient, and the column density of the species emitting the observed radiation. However, the parameters driving the underlying physics, such as the FUV flux, are not easily constrained using only LVG modeling, and abundances must be assumed in order to derive the mass of the molecular gas. In-order to constrain the FUV flux, in star-forming regions, PDR modeling is usually used where the FUV flux is an important source of heating. Observations of luminous (LIRGS: $L_{IR}$ (8-1000 $\mu$m) $\sim 10^{11}$ $L_\odot$ ) and ultra-luminous (ULIRGs: $L_{IR} \sim 10^{12}$ $L_\odot$) infra-red galaxies, that are a sub-class of star-forming galaxies, can not be modeled using PDR models alone, since PDR models are not able to fully match the observed atomic and molecular line intensity ratios (e.g. Loenen et al. 2008). XDRs models provide an alternative approach in modeling the emission of LIRGS and ULIRGS in a more satisfactory manner (e.g. Meijerink et al. 2007) but in some cases these models are not consistent with the required X-ray fluxes in AGN (for e.g. Maloney et al. 1996b, Papadopoulos 2010, Meijerink et al. 2011, Rosenberg et al. 2014a,b).

In this thesis we explore how mechanically heated PDR models can be used to solve this problem by matching the observed line ratios. We will also use such models to constrain the amount of mechanical heating needed and find a diagnostic for it.

## 1.5 Thesis outline

The work presented in this thesis is divided into two parts. In the first part a parametric study of PDRs is performed to probe the effect of mechanical heating under different physical conditions and to identify possible diagnostics for mechanical feedback. In the second part, the PDR models of this parametric study are applied to galaxy models to produce emission maps of molecular species and analyze them. More specifically, the work done in each chapter is as follows.

In **Chapter 2** the effect of mechanical heating on the thermal and chemical properties of PDRs is investigated; in particular, the effect on the kinetic temperature of the gas, abundance, column density, as well as column density ratios of the molecular species CO, HCN, HNC, $HCO^+$and $H_2O$ are studied.

We solve the equilibrium state of all model clouds by using the Leiden PDR-XDR code developed by Meijerink & Spaans (2005). In this code the PDR region irradiated from one side by a FUV source is discretized into 1D semi-infinite parallel zones (slabs). The chemical and thermal properties of the zones are solved for iteratively at equilibrium. An escape probability formalism is used to treat the radiative transfer through the discretized slabs. The full internal details of the code are described by Meijerink & Spaans (2005) and the optimization details are discussed in the methods section of Chapter 2. Most possible conditions of the interstellar medium relevant to galaxies are covered by the parameter space of the PDR models. The grids of the models include hydrogen gas density ($1 < n < 10^6$ cm$^{-3}$), FUV radiation field ($0.32 < G_0 < 10^6$) measured in so-called Habing units, $G_0$, and mechanical heating rate ($10^{-24} < \Gamma_{\rm mech} < 10^{-16}$ erg cm$^{-3}$ s$^{-1}$).

The chemical and thermal properties of clouds determine the radiation emanating from them. In **Chapter 3** we extend the work done in the previous chapter by investigating the effect of mechanical heating on atomic and molecular lines, and their ratios. We try to use those ratios as a diagnostic to constrain the amount of mechanical heating in a region and also study its significance on estimating the $H_2$ mass. The emission of the PDR grids are computed assuming the Large Velocity Gradient approximation where the equilibrium state of the PDR models is used as input to RADEX (van der Tak et al. 2007) where the emission is computed in post-processing mode.

Emission of CO(1-0) is ubiquitously detected in galaxies and is commonly used to estimate the molecular mass in a galaxy or giant molecular cloud (Solomon et al. 1987, Bolatto et al. 2013, and references therein). In **Chapter 4**, we study the effect of mechanical heating on diagnostic line ratios of CO and $^{13}$CO in model galaxies. In particular we determine whether these diagnostic line ratios can be used to probe the presence and constrain the magnitude of mechanical heating in actual galaxies. We make use of the PDR models of Chapter 3 and apply them to the gas of a simulated disk and dwarf galaxy in post-processing mode and produce emission maps for the rotational transitions of the CO molecule and its $^{13}$CO isotopologue up to $J = 4-3$. The disk and dwarf galaxies are simulated using solar and $1/5$ solar metallicities. The emission maps of these model galaxies are used to compute line ratio maps of the CO and $^{13}$CO transitions. These maps are used to illustrate the effect of mechanical feedback on the physical parameters obtained from the molecular line intensity ratios.

In **Chapter 5** we extend the work of the previous chapter to species other than CO and $^{13}$CO. We include rotational transitions with critical densities $n \gtrsim 10^4$ cm$^{-3}$, for instance $4-3 < J \leq 15-14$ transitions of CO and $^{13}$CO, also $J \leq 7-6$ transitions of HCN, HNC and HCO$^+$. In this chapter, we focus only on the disk galaxy, where the density field of the interstellar medium of the model galaxy is re-sampled to account for the lack of resolution and for the emission of gas with densities $> 10^3$ cm$^{-3}$. The re-sampling is done by assuming that the probability density function (PDF) of the density is a log-normal function inferred from the resolved low density scales. Following a similar approach as in Chapter 4, we fit the line-ratios of the synthetic emission maps for the central 2 kpc of the galaxy using one model PDR.

Furthermore, in the second part of this chapter, we investigate the impact of different log-normal density PDFs on the distribution of the luminosity as a function of density. The aim of this exercise it to check the conditions under which significant emission is obtained from gas with densities $n > 10^4$ cm$^{-3}$, and to test for the possibility of constraining the PDF using line ratios of high density tracers. In super-sonically turbulent clouds the Mach number, $\mathcal{M}$, is related to the dispersion of a log-normal distribution. We use this relationship to estimate the Mach number of the ISM by constraining the parameters of the density PDF using molecular line emission intensity ratios.

In the final chapter we put the work done in the thesis into the perspective of recent observations by the *Herschel* Space Observatory (Pilbratt et al. 2010) and discuss the importance and possible applications of our models to data obtained with Atacama Large Millimeter Array[4] (ALMA). We also discuss the major caveats of our present modeling and ways of improving future modeling, the limitations and some estimates on the requirements for improved modeling of the chemistry and the radiative transfer.

[4] http://www.almaobservatory.org/